

Diverse cell stresses induce unique patterns of tRNA up- and down-regulation: tRNA-seq for quantifying changes in tRNA copy number

Yan Ling Joy Pang¹, Ryan Abo², Stuart S. Levine² and Peter C. Dedon^{1,*}

¹Department of Biological Engineering and Infectious Diseases Interdisciplinary Research Group, Singapore-MIT Alliance for Research & Technology, Massachusetts Institute of Technology, Cambridge, MA 02139, USA and

²Department of Biology, Massachusetts Institute of Technology, Cambridge, MA 02139, USA

Received August 25, 2014; Revised September 16, 2014; Accepted September 27, 2014

ABSTRACT

Emerging evidence points to roles for tRNA modifications and tRNA abundance in cellular stress responses. While isolated instances of stress-induced tRNA degradation have been reported, we sought to assess the effects of stress on tRNA levels at a systems level. To this end, we developed a next-generation sequencing method that exploits the paucity of ribonucleoside modifications at the 3'-end of tRNAs to quantify changes in all cellular tRNA molecules. Application of this tRNA-seq method to *Saccharomyces cerevisiae* identified all 76 expressed unique tRNA species out of 295 coded in the yeast genome, including all isoacceptor variants, with highly precise relative (fold-change) quantification of tRNAs. In studies of stress-induced changes in tRNA levels, we found that oxidation (H₂O₂) and alkylation (methylmethane sulfonate, MMS) stresses induced nearly identical patterns of up- and down-regulation for 58 tRNAs. However, 18 tRNAs showed opposing changes for the stresses, which parallels our observation of signature reprogramming of tRNA modifications caused by H₂O₂ and MMS. Further, stress-induced degradation was limited to only a small proportion of a few tRNA species. With tRNA-seq applicable to any organism, these results suggest that translational control of stress response involves a contribution from tRNA abundance.

INTRODUCTION

Transfer RNA (tRNA) is the primary molecular species tasked with reading the amino acid-coding sequences in mRNA during translation. Its function is controlled at a va-

riety of levels including differential expression and maturation of each isoacceptor (1), decoration with dozens of different post-transcriptional ribonucleoside modifications (2) and selective degradation of specific tRNAs for quality control and signaling (1,3–7). While individual tRNA modifications are known to affect tRNA stability as well as translational fidelity and efficiency (8), emerging evidence points to a systems-level control of tRNA function in translational control of cell phenotype and cellular responses to stress and stimuli (9–12), with potential roles for both the spectrum of tRNA modifications and the number of copies of individual tRNA molecules. For example, we have demonstrated that cells respond to different stresses by uniquely reprogramming tRNA wobble modifications to cause selective translation of mRNAs containing biased use of the cognate codons, with different families of codon-biased genes expressed for each different stress (9–11,13). The caveat here is that a change in the level of a tRNA modification could result from either altered activity of a tRNA-modifying enzyme or a change in the number of copies of the tRNA species harboring the modification, or both. Similarly, there is evidence for degradation of specific tRNA species as part of stress response and quality control pathways (3–7), but the effect of the degradation phenomena on the entire population of tRNA species is not clear.

While the ability to quantitatively monitor tRNA abundance changes in cells is critical to understanding translational control mechanisms, there are few methods for quantifying tRNA species, other than traditional northern blots, and current methods are hampered by limited coverage and lack of quantitative depth. Microarray-based methods have proven useful for quantifying a subset of all tRNA species in specific prokaryotes and eukaryotes (14,15). However, this technology requires custom-made arrays for each organism, does not provide complete coverage of all tRNA species (e.g. isodecoders), and has a limited dynamic range for quantification. A limitation of microar-

*To whom correspondence should be addressed. Tel: +617 253 8017; Fax +617 324 7554; Email: pcedon@mit.edu

Disclaimer: The views expressed herein are solely the responsibility of the authors and do not necessarily represent the official views of the National Research Foundation of Singapore. The funders had no role in study design, data collection and analysis, decision to publish or preparation of the manuscript.

ray technology is demonstrated by the detection of only 39 of the 56 unique cytoplasmic tRNA species expressed from 273 genes in *Saccharomyces cerevisiae* (16,17). As another example of RNA quantification, the original development of small RNA-seq and RNA-seq (18) has been employed as a means to profile small RNAs (<40 nucleotides) and mRNAs (19,20), but the technology has not been explored with tRNA specifically. Furthermore, neither microarrays nor high-throughput RNA sequencing technologies have been assessed for the effect of dynamically changing modified ribonucleosides on the quantitative rigor of the methods.

To solve these problems and test the hypothesis of stress-induced reprogramming of tRNA copy numbers, we developed a comprehensive method for quantifying changes in the levels of all expressed tRNA species based on next-generation sequencing. The critical feature of this tRNA-seq method involves ligation of a defined-sequence linker to only the 3'-end of purified tRNA, of which the first ~30 nucleotides (nt) provide unique identification of all tRNAs and contain the fewest modified ribonucleosides along the length of most tRNAs. This minimizes modification-induced polymerase fall-off during reverse transcription to generate a set of cDNAs that is then subjected to another round of linker ligation at the new 3'-end, followed by polymerase chain reaction (PCR) amplification and subsequent standard next-generation sequencing. Unlike standard RNA-seq, in which both 5' and 3' DNA adaptors are ligated simultaneously before reverse transcription (21), this two-step ligation approach not only minimizes modification-induced polymerase fall-off but also captures truncated fragments formed if reverse transcription terminates at modified ribonucleosides, with enough sequence to identify the tRNA. This ensures that even highly modified tRNAs can be quantified in spite of premature polymerase fall-off. In applications of the method to *S. cerevisiae*, the large dynamic range of next-generation sequencing reads (22) enabled identification and quantification of all expressed unique tRNAs in a single experimental run. Analysis of stress-induced changes in tRNA levels revealed that oxidation and alkylation stresses did not alter the number of copies of more than half of the tRNA species, with nearly identical patterns of up- and down-regulation of other tRNA species, which is contrary to the signature reprogramming of tRNA modifications caused by these stresses (10,11). Further, quantitatively insignificant stress-induced degradation was limited to only a small proportion of a few tRNA species, with no global or widespread degradation of tRNAs observed. This is consistent with the conclusion that the majority of truncated reads represent full-length tRNAs that were shortened due to polymerase fall-off. These results attest to the utility tRNA-seq in understanding mechanisms of translational control of gene expression, with the method broadly applicable to any organism.

MATERIALS AND METHODS

Exposure of *S. cerevisiae* cultures

Mid-log phase cultures of wild-type *S. cerevisiae* BY4741 were exposed for 1 h to 0.25 mM hydrogen peroxide (H₂O₂) or 10 mM methyl methanesulfonate (MMS) resulting in

50% cell survival compared to unexposed cells. This was followed by centrifugation at 6500 × g for 15 min. The cytotoxic sensitivity of *S. cerevisiae* to the toxicants was assessed by exposing mid-log phase cultures to various concentrations of toxicant ranging from 0 to 1.5 mM H₂O₂ or 0 to 25 mM MMS for 1 h, followed by plating a dilution of cells at each toxicant concentration on yeast-peptone-dextrose (YPD) agar to determine viability.

Isolation and purification of *S. cerevisiae* tRNA

A total of 18 cultures (25 ml) of BY4741 *S. cerevisiae* were prepared (6 unexposed, 6 H₂O₂-exposed, 6 MMS-exposed). Following toxicant exposure resulting in 50% survival, tRNA-containing small RNA species were isolated using an Invitrogen PureLink miRNA kit. Further purification of tRNA from the small RNA eluent was carried out on a 1200 Agilent HPLC system fitted with an Agilent size-exclusion SEC3 column eluted under isocratic conditions at 60°C with 8 mM ammonium acetate (23). The purified tRNA was quantified by UV absorbance at 260 nm.

Reverse transcription of tRNAs

Purified tRNA was first denatured at 80°C for 5 min followed by cooling on ice. The 3'-ends of all tRNAs were ligated to pre-adenylated 20 nt DNA linkers with a 3'-dideoxy end (DNA linker 1: /5'rApp/TTTAACCGCGAATTCCAG/3'ddC/). Ligation reactions were carried out at 16°C for 18 h in the presence of 3 µg of T4 RNA ligase 2 (truncated) using a 1:2 ratio of tRNA:DNA linker. The resulting ligation products were purified by high-performance liquid chromatography (HPLC) and reverse transcribed using 200 units of Primescript reverse transcriptase. After HPLC purification of the reverse transcribed products, the resulting cDNA was subjected to a second ligation step to attach a 19 nt pre-adenylated DNA linker with a 3'-dideoxy to the 3'-end of the cDNA (DNA linker 2: /5'rApp/CACTCGGGCACCAAGGA/3'ddC/). This was performed at 4°C for 18 h with a cDNA:DNA linker ratio of 1:2 and in the presence of 20 units of T4 RNA ligase 1. The products from the second ligation reaction were HPLC purified before undergoing PCR amplification. Finally, the PCR-amplified cDNA was cleaned up on the HPLC before being processed on an SPRI-works (Beckman Coulter) system, with the ends blunt-ended via fill-in reactions and exonuclease activity. The cDNA was then ligated to Illumina-specific sequencing adaptors harboring unique sequencing primer hybridization sites. For multiplexed Illumina sequencing, 5-mer index sequences were incorporated at one end of the cDNA next to the Illumina adaptors. The paired-end library was enriched before being sequenced on the Illumina HiSeq at the MIT BioMicro Center. The location of each barcode was recorded and this tag allowed for the post-sequencing identification of each population.

Quantification and statistical analysis of tRNA fold-changes in response to stress

The 295 *S. cerevisiae* tRNA sequences were first obtained from the GtRNadb (24). The tRNA sequences were pro-

cessed to collapse the highly similar tRNAs to a unique set of sequences for each species, resulting in 76 unique *S. cerevisiae* tRNA sequences. Prior to mapping, the adapter sequence was removed from sequence reads and sequences > 10 bp were then aligned to tRNA sequences using BLAT (25) with default parameters. All reads mapping to a single isoform were considered in the analysis, while reads mapping to multiple different isoforms were discarded. Five tRNAs comprising tRNA^{Gly}(GCC), tRNA^{Gly}(UCC), tRNA^{His}(GUG), tRNA^{Ser}(AGA) and tRNA^{Cys}(GCA) had significantly higher reads than others, possibly due to ligation or polymerase biases. These 'jackpot' tRNAs were excluded from all further analyses.

edgeR software was used to detect statistical differences in expression of tRNA between conditions (26). edgeR was designed to perform differential abundance analysis for 'count-based' data modeled using a negative binomial distribution with an estimated dispersion parameter. The *S. cerevisiae* tRNA sample counts were first normalized for varying library sizes using the calcNormFactors function. Different expressions between all pairwise conditions for tRNAs were tested using generalized linear model likelihood ratio tests.

Hierarchical clustering analysis was performed with Cluster 3.0 using the centroid linkage algorithm based on the distance between each dataset measured using Pearson correlations. Java Treeview was used to represent the data in heat map format. Multivariate data analysis was performed using SIMCA-P+ (Umetrics, Kinnelon).

Northern blot analysis

Purified total tRNA (1 µg) was spotted onto a nylon membrane (Millipore) and cross-linked by UV irradiation (254 nm, 2 min). The membrane was treated with ULTRAhyb-Oligo hybridization buffer (Life Technologies) followed by hybridization of the blot with a tRNA-specific DNA probe that was ³²P-labeled on the 5'-end with [γ -³²P]ATP (6000 Ci/mmol, 10 µCi/µL) (PerkinElmer) and T4 polynucleotide kinase. For H₂O₂ exposure studies, tRNAs including tRNA^{Gly}(UCC), tRNA^{Glu}(CUC), tRNA^{Ile}(AAU), tRNA^{Thr}(UGU), tRNA^{Leu}(UAA), tRNA^{Arg}(UCU) and tRNA^{Asp}(GUC) were analyzed, while tRNA^{Gly}(UCC), tRNA^{Ile}(AAU), tRNA^{Leu}(UAA) and tRNA^{Asp}(GUC) were analyzed for MMS exposure studies. The blot was washed extensively after hybridization and the ³²P intensity in the dried blot recorded by phosphorimager analysis (18 h exposure).

RESULTS

tRNA processing workflow

As shown in the workflow in Figure 1, this tRNA-seq method takes advantage of the paucity of modified ribonucleosides at the 3'-ends of tRNAs with a two-step ligation strategy. Starting with either isolated small RNA species (<200 nt), as derived from most small RNA extraction kits, or tRNA purified by gel electrophoresis (10) and HPLC (23), the first step involves ligating the 3'-end of the tRNA to a DNA linker harboring a 3'-dideoxynucleotide, followed

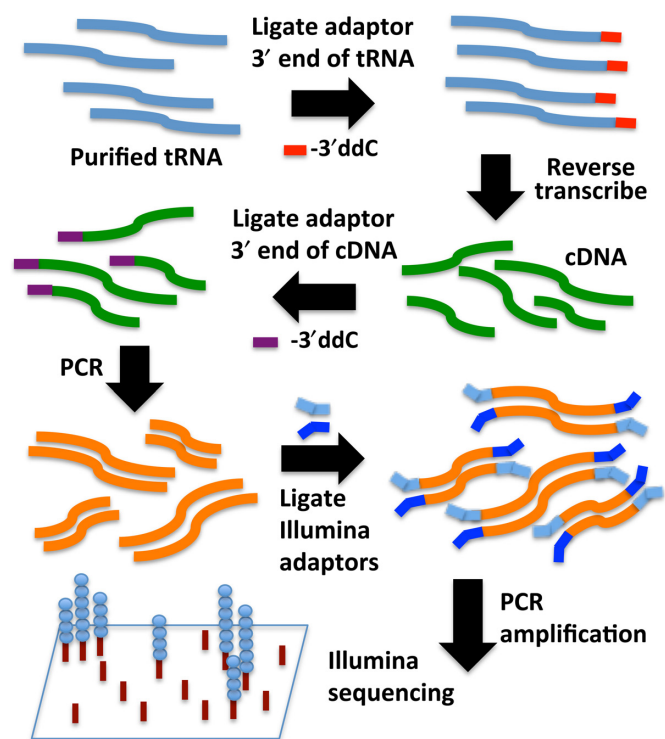


Figure 1. Two-step ligation method for the conversion of tRNA to cDNA. Bulk tRNAs extracted from *S. cerevisiae* are first 3'-end ligated with a DNA adaptor. After reverse transcription, a second DNA adaptor is ligated to the 3'-end of the resulting cDNA, and the resulting species are PCR amplified followed by standard Illumina sample preparation and analysis.

by reverse transcription in bulk using a primer complementary to the DNA linker. The cDNA is then subjected to a second 3'-end ligation with a different DNA linker followed by PCR amplification using primers complementary to the tagged 3'- and 5'-ends (Figure 1). The last step involves processing of the amplified cDNA for next-generation sequencing. In the present studies, we used the Illumina sequencing platform, which required standard Illumina sample preparation protocols to create a barcoded, paired-end library using Illumina primers.

tRNA-seq read length, alignment, coverage and statistics

The uniquely barcoded libraries derived from either HPLC-purified total tRNA or small RNA populations were subjected to multiplex sequencing using either the Illumina HiSeq 2000 or Illumina MiSeq system to read 40 or 70 nt in from a single end, respectively. The total number of raw reads ranged from 50 to 220 million on the HiSeq 2000 and 6 to 7 million reads on the MiSeq, with the distribution of read counts from purified tRNAs sequenced on HiSeq 2000 shown in Supplementary Figure S1. The sequence alignment program BLAT (25) was used with default settings to align all raw sequencing reads greater than 10 nt. This analysis resulted in identification of all 76 unique *S. cerevisiae* tRNAs (including mitochondrial tRNAs) present in the GtRNAdb tRNA database (24), with identities established for both isoacceptor tRNAs and for isodecoders (27) (i.e. isoacceptor tRNA species that differ in sequence other than

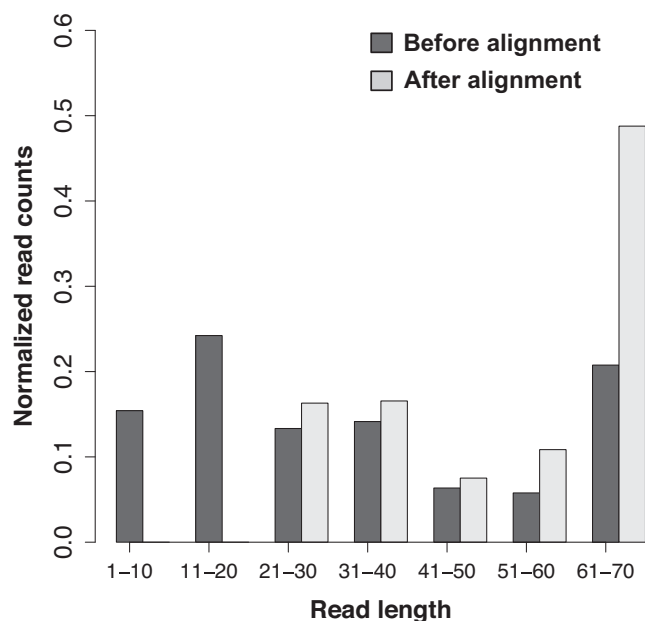


Figure 2. Distribution of read lengths of untreated total small RNA. Normalized read counts (as proportion of total reads) from MiSeq analysis of total small RNA from unexposed cells were binned according to their read lengths before alignment of uniquely assignable sequences (dark gray bars) and after alignment (light gray bars).

the anticodon) (24,28). A scoring system that accounted for polymerase-induced mismatches and gap penalties, such as those caused by modified ribonucleosides, was used during alignment and only sequence alignments with a minimum score of 30 were counted in the sequencing analysis. Using previously published computational methods (29), we considered only reads that mapped to a single tRNA isoform (i.e. unique member of an isoacceptor group) and discarded reads mapping to multiple tRNA isoforms. While this collapsed the number of applicable reads to 12–149 million and 1–5 million on HiSeq 2000 and MiSeq, respectively (Supplementary Table S1), it ensured that each sequencing read mapped only to one specific tRNA, which is essential for rigorous relative quantification of individual tRNA species. Since the reliable identification of a unique tRNA species requires more than ~20 nt of sequence information, we computed the average read length distribution on the Illumina MiSeq for total small RNA from unexposed cells before alignment and compared the data to the resulting read length distribution after alignment (Figure 2). This analysis revealed that a significant proportion of sequenced total small RNAs were shorter than 20 nt, possibly representing degradation products of larger non-coding RNA species (including tRNA) and tRNA fragments generated as a result of termination of reverse transcription by polymerase fall-off. RNA species <20 nt could not be reliably assigned to a single specific tRNA isoacceptor and were discarded. After alignment of uniquely assignable sequences, the majority of tRNA sequences were 61–70 nt in length, which most likely represents full-length tRNA since we chose to use a sequencing length of 70 nt on the MiSeq platform (Figure 2). Mutations caused

by polymerase-induced mispairings at sites of modified ribonucleosides are unlikely to affect the read count for a tRNA sequence since the data analysis scoring system provides a mismatch tolerance in the assignment of sequence identities to individual tRNA species. Considering all of these parameters and the presence of five extremely highly amplified tRNA species, we were able to detect 41 cytosolic isoacceptor tRNA species that parsed into 56 total cytosolic tRNA species at the level of isodecoders, and 20 mitochondrial tRNAs. Included in this count were six isodecoders, five cytosolic isodecoders (tRNA^{Asp}(GUC), tRNA^{Glu}(UUC), tRNA^{Lys}(CUU), tRNA^{Tyr}(GUA) and tRNA^{Val}(AAC)) and one mitochondrial isodecoder (tRNA^{Met}(CAU)), which could not be quantified by sequencing because they differed by only a few bases and sequencing read counts could not accurately distinguish them. We were thus able to detect all expressed tRNAs over a range of 0.8–242 000 counts per million (Supplementary Table S2) and we used changes in read counts for 76 tRNA sequences to calculate relative fold-change values in tRNA expression levels between populations.

Several features of tRNA quantitation emerged from statistical analyses of the HiSeq 2000 sequencing reads derived from tRNA purified from cells subjected to three treatment conditions (untreated, H₂O₂ and MMS; see below). The tRNA-seq data proved to be highly precise in terms of reproducibility, which allows significant distinctions among small changes in tRNA abundance. The read counts obtained from HiSeq and MiSeq for each tRNA species in samples of purified tRNA (Supplementary Table S2) were subjected to pairwise correlation analysis between individual biological replicates, with the resulting Pearson correlation coefficients shown in Supplementary Figure S2. This analysis revealed strong correlations among the datasets, with *r*-values for replicate libraries ranging from *r* = 0.95 to 1.0 and *r* = 0.74 to 0.99 for samples run on HiSeq 2000 and MiSeq, respectively. The precision of the data was also high, with average coefficients of variation for six biological replicates of the purified tRNA of 0.47 ± 0.17, 0.39 ± 0.17 and 0.36 ± 0.15 for unexposed, H₂O₂-exposed and MMS-exposed samples, respectively, and for the total small RNA of 0.26 ± 0.13, 0.17 ± 0.07 and 0.38 ± 0.31, respectively, as sequenced on the HiSeq 2000 (Supplementary Table S2). The relatively low variance among biological replicates from each exposure group enabled statistically significant (*P* < 0.05) relative quantification of stress-induced changes in tRNA levels down to 1.4-fold, as discussed shortly.

While the highly precise read count data provide sensitive quantification of changes in the levels of individual tRNA species between samples, there was large variation in the read count data among the individual tRNA species in each sample. These variations likely arose from variable ligation efficiencies for the different RNA sequences (30,31). For example, five of the tRNAs (tRNA^{Gly}(GCC), tRNA^{Gly}(UCC), tRNA^{His}(GUG), tRNA^{Ser}(AGA) and tRNA^{Cys}(GCA)) had extremely high read counts compared to the other tRNAs and were arbitrarily defined as ‘jackpots.’ However, as with other tRNAs, the read counts for these five tRNAs were highly precise. Comprising 8–21% of the total number of sequencing reads in a run, tRNA^{Gly}(GCC), tRNA^{Gly}(UCC), tRNA^{His}(GUG),

tRNA^{Ser(AGA)} and tRNA^{Cys(GCA)} contributed $21\% \pm 3\%$, $13\% \pm 2\%$, $8\% \pm 1\%$, $15\% \pm 3\%$ and $14\% \pm 3\%$ of the total reads, respectively. The read counts for the remaining 71 tRNAs ranged from 0.0001% to 2.7% of the total number of sequencing reads per run (Supplementary Figure S1). While limiting absolute quantification of tRNAs, this variation does not affect highly precise relative quantification.

tRNA copy number changes in response to cytotoxic stresses

The high precision of the tRNA-seq data provides a means to explore a mechanistically informative landscape of relative changes in tRNA copy number at a systems level under different cell stresses and environmental changes. We previously showed that cells respond to different stresses by uniquely changing the relative quantities of tRNA modifications, with this reprogramming causing selective translation of codon-biased mRNAs (9–11,13). However, variations in the levels of tRNA modifications could be caused by both altered enzyme activity and by changes in tRNA levels. To explore the effects of cell stress on tRNA abundance, we applied tRNA-seq to *S. cerevisiae* exposed to equitoxic doses (LD₅₀) of hydrogen peroxide (H₂O₂) and methylmethanesulfonate (MMS), two stresses shown previously to evoke highly different tRNA modification changes and translational responses (9–11). Using HiSeq 2000 sequencing of purified tRNA, we performed an untargeted analysis of read counts (Supplementary Table S2) derived from all 76 unique tRNAs in *S. cerevisiae*, with the read counts normalized for varying library sizes and with differential expression levels between all pairwise conditions for tRNAs tested using generalized linear model likelihood ratio tests. Average fold-change data for each of the 76 tRNA species under the two treatment conditions are shown in Supplementary Table S3 and analyzed by hierarchical cluster analysis in Figure 3. The tRNA-seq data reveal that neither stress caused significant changes ($P < 0.1$) in the levels of more than 50% of the tRNAs, while levels varied by less than 4-fold for those tRNAs for which either stress caused a significant change. Hierarchical cluster analysis revealed strikingly consistent up- or down-regulation for all but 18 of the tRNAs, with the 18 tRNAs showing opposing changes for the H₂O₂ and MMS exposures (Figure 3).

We next used a northern dot-blot assay to validate the sequencing-derived fold-change data for stress-induced changes in tRNA copy numbers: tRNA^{Gly(UCC)}, tRNA^{Glu(CUC)}, tRNA^{Ile(AAU)}, tRNA^{Thr(UGU)}, tRNA^{Leu(UAA)}, tRNA^{Arg(UCU)} and tRNA^{Asp(GUC)} for tRNAs affected by H₂O₂ exposure, and tRNA^{Gly(UCC)}, tRNA^{Ile(AAU)}, tRNA^{Leu(UAA)} and tRNA^{Asp(GUC)} for MMS exposure. These representative tRNAs were chosen since they were subject to toxicant-induced changes in copy number by tRNA-seq and they had unique 3'-end sequences to prevent cross-hybridization of the probes. Fold-change values computed from the Illumina HiSeq data were plotted against the values determined by dot-blot analyses (Supplementary Figure S3). The plot revealed a significant and strong correlation between the datasets, with a Pearson correlation coefficient of $r = 0.84$, $P < 0.001$.

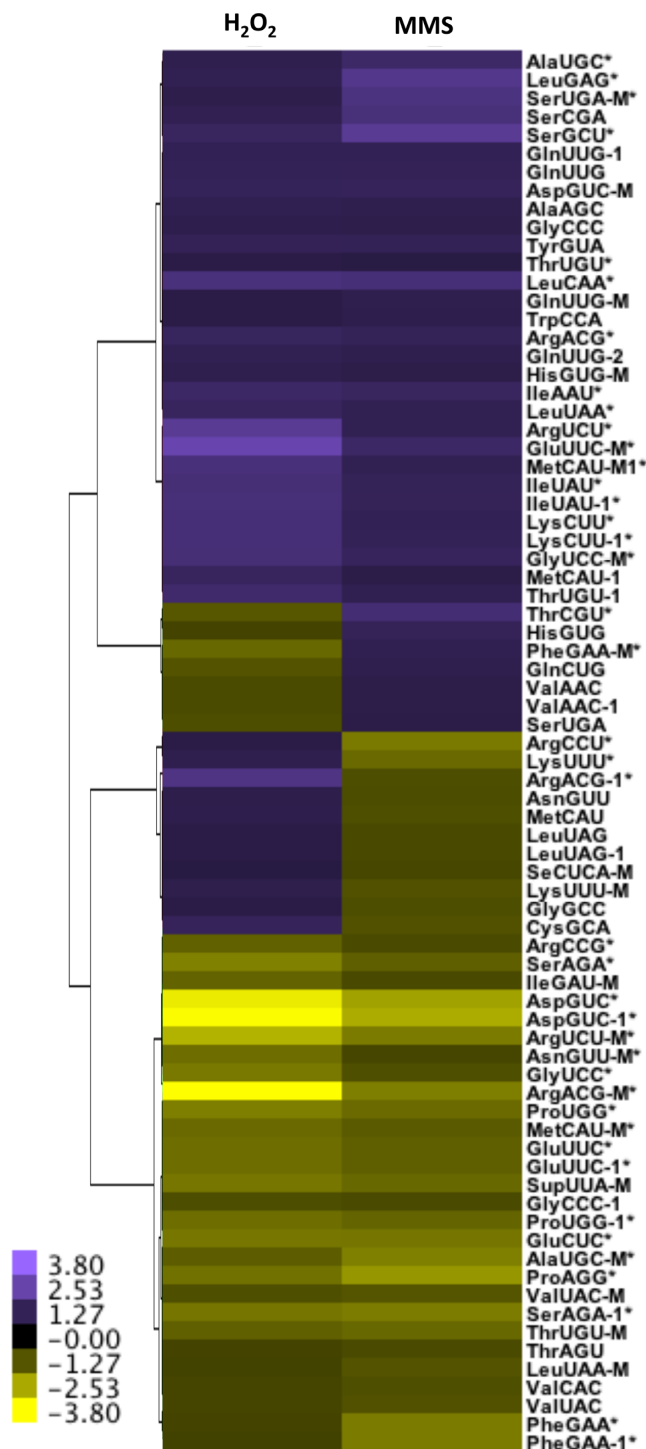


Figure 3. Hierarchical cluster analysis of either H₂O₂ or MMS induced changes in tRNA expression levels in cells. Expression levels of tRNAs extracted from either H₂O₂- or MMS-exposed cells were calculated from tRNA-Seq and compared to control tRNAs from untreated conditions. Hierarchical cluster analysis was performed on fold-change data. The bottom left color bar indicates the range of fold-change values. Asterisks denote significant changes at $P < 0.1$ in at least one exposure condition as determined by Student's t-test.

High reverse transcription error rates variably correlate with tRNA modification sites

Another potential application of tRNA sequencing entails mapping the locations of modified ribonucleosides based on modification-induced polymerase errors (19,32). Using data generated from MiSeq analysis, we analyzed misincorporation error rates during sequencing of tRNAs from the set of control (unexposed) and H₂O₂- and MMS-exposed cells. The assumption here is that the major source of mismatch error involves the reverse transcription step. We observed average sequencing error rates of 3.4–3.8%, with tRNAs extracted from toxicant-exposed cells exhibiting significant increases in guanine mismatches (Supplementary Figure S4). In tRNA from unexposed cells, error rates for A, C, T and G were 4.0%, 3.1%, 0.5% and 6.0%, respectively, which are significantly higher than previously published error rates of $\leq 0.1\%$ for MiSeq (19,33). The high error rates and the fact that the majority of tRNA reads were 61–70 nt in length (70 nt sequencing limit) suggest that the reverse transcriptase was able to read most modified ribonucleosides, albeit incorrectly, and process past the modifications to produce a full-length transcript.

In terms of using polymerase-induced errors to localize modified ribonucleosides in tRNA, we were able to correlate a high mismatch frequency with the known location of N²,N²-dimethylguanosine (m²G) and changes in mismatch frequency correlating with stress-induced changes in m²G levels (10,11). m²G is found predominantly at position 26 of *S. cerevisiae* tRNAs and is known to cause reverse transcription errors (19). We examined position 26 in the sequencing data for unexposed cells and found an overall 27% mismatch frequency involving misreading m²G as T, A and C (19.8%, 5.1% and 1.7%, respectively). Stress-induced changes in the error rate at m²G sites increased with H₂O₂ exposure and decreased for MMS (Figure 4), which is consistent with our previous observations for changes in the level of m²G with both of these stresses (11). Similarly, another modification, 2'-O-methylcytidine (Cm), showed mismatch rates consistent with stress-induced changes in the levels of those modifications from previous studies (11), but did not reach significant levels in our analysis. On the other hand, analysis of mismatch frequency at other tRNA sites known to be modified with N⁷-methylguanosine (m⁷G) and N¹-methyladenosine (m¹A), for example, revealed that changes in mismatch frequency due to exposure to stress conditions did not correlate with previous observations for stress-induced changes in the levels of those modifications (11). There is little information about modification-induced mismatch behavior of reverse transcriptases in general, and the Primescript reverse transcriptase specifically, which limits the utility of tRNA-seq for mapping modified ribonucleosides based on mismatch rates. Furthermore, the approach is likely to be influenced by the read length of sequencing. For example, read lengths shorter than the full length of tRNA will provide only partial mismatch information and subsequently biased mismatch data. More information is needed to establish empirical rules for reverse transcriptase responses to modified ribonucleosides.

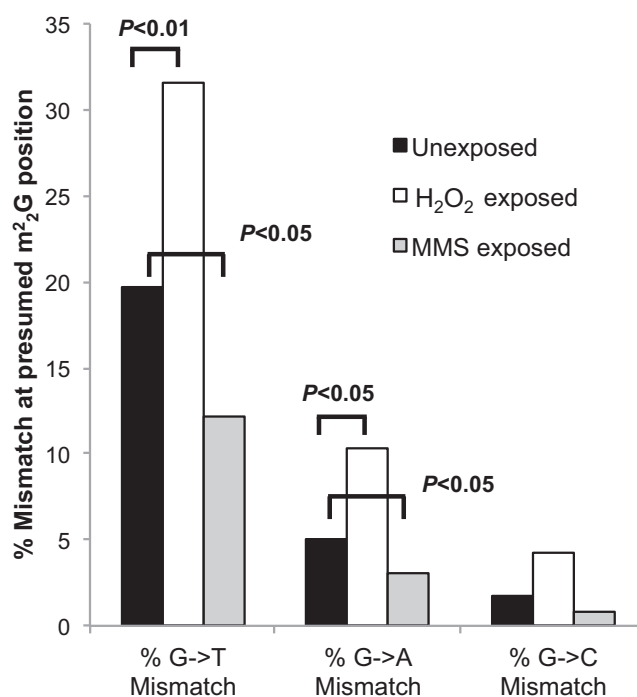


Figure 4. Mismatch rates at m²G sites in *S. cerevisiae* tRNA. The mismatch error rate in tRNAs known to possess the modified base m²G at position 26 was quantified from tRNA-seq data for control (black bars), H₂O₂-exposed (white bars) and MMS-exposed (gray bars) cells. Data represent mean \pm SD for six biological replicates, with *P* values determined by Student's *t*-test; SD: standard deviation.

Quantifying stress-induced tRNA degradation by tRNA sequencing

Given the emerging role of tRNA cleavage and degradation in RNA quality control, stress response and signaling (3–7,34–36), we explored the utility of tRNA sequencing for quantifying tRNA fragmentation by one of the known tRNA degradation pathways (3,4) that involves ribonuclease digestion at the anticodon loop in response to oxidation and alkylation stresses. The tRNA sequencing data from MiSeq were pooled by fragment length into bins of 21–30, 31–40, 41–50, 51–60 and 61–70 nt (70 nt maximal read length), which provided a means to quantify fragmentation by analyzing sequences in these size ranges. Consistent with previous observations that the amount of full-length tRNA did not decline significantly in stress-induced degradation pathways (37), our analysis of tRNA fragments in samples of total small RNA from untreated, H₂O₂-treated and MMS-treated cells showed no significant (*P* < 0.05) stress-induced changes in abundance of fragments in any size range (Supplementary Figure S5a). These results allow us to conclude that there is no wholesale degradation of tRNA species in the response to oxidation and alkylation stresses. Since we did not observe any extensive degradation of tRNAs in response to stress, it is likely that the vast majority of sequencing reads represent full-length transcripts and shorter reads are likely due to polymerase fall-off at modified bases.

However, there were several notable trends in tRNA fragmentation that warrant further study. For example, many of

the tRNAs show a non-significant ($P > 0.1$) spike in fragments, such as the H_2O_2 -induced 1.4-fold increase in 31–40 nt fragments from tRNA^{Met(CAU)} (Supplementary Figure S5b). While this is consistent with previous studies showing that oxidative stress leads to generation of ~30–40 nt tRNA fragments by cleavage at the anticodon loop (4), the fact that the changes do not rise to the level of statistical significance points to the limit of quantitation of the tRNA-seq method due to possible inherent biases occurring at the ligation and amplification steps of sample preparation. More recently, evidence has emerged for the sequence of steps in stress-induced tRNA degradation, with initial cleavage at the 3'-end of the tRNA to cause deacylation followed by cleavage into tRNA halves (38). It is thus possible that longer exposure times are necessary to observe any statistically significant change in overall tRNA quantities. Similarly, analysis of the recently identified 17–26 nt tRNA-derived fragments (tRFs) (21,34,39) showed fragments corresponding to tRNA^{Lys(CUU)} and tRNA^{Asp(GUC)} in *S. cerevisiae* (37), which is consistent with our observation that tRNA^{Lys(CUU)} and tRNA^{Asp(GUC)} showed a larger 21–30 nt fragment pool (i.e. potential tRFs) in sequencing samples derived from total small RNA species compared to HPLC-purified tRNA (Supplementary Figure S5c). It is noteworthy that some of the most abundant tRFs (21,34,39) appear as 'jackpot' tRNAs in our sequencing analysis, which raises questions of artifact in the quantification of the tRFs.

DISCUSSION

Based on application of this new tRNA-seq method, we conclude that, while distinct oxidation and alkylation stresses induce nearly identical patterns of up- and down-regulation for most tRNAs, the cellular response to these stresses involves unique changes in the levels of several tRNA species. This parallels our observation of signature reprogramming of tRNA modifications caused by H_2O_2 and MMS (9–11,13) and suggests that tRNA copy number plays a role in controlling selective translation of stress response genes (9–11,13). Further, stress-induced degradation was limited to only a small proportion of a few tRNA species, which supports the idea that cells do not respond to stresses by wholesale removal of tRNA species from the tRNA pool for either quality control or altered translation patterns. We arrived at these conclusions using a combination of molecular and bioinformatic tools to develop a sequencing-based method to precisely quantify relative changes in tRNA abundance in cells. As a result of the millions of reads provided by next-generation sequencing technology (22), the method is comprehensive in detection and relative quantification of all 76 expressed tRNA species in *S. cerevisiae* over a million-fold dynamic range. While there is established sequencing technology for profiling miRNA and mRNA (40–42), sequencing analysis of tRNA has been hampered by the unique problem of highly abundant modified ribonucleosides comprising up to 10% of the nucleotide content of a tRNA molecule, with the modifications causing mutations or terminating reverse transcriptase activity (19,43). We minimized this modification problem with a two-step ligation process in which only one end of the tRNA is ligated with an adaptor before reverse transcrip-

tion. The 3'-end of tRNA was chosen as the site for the first ligation due to the paucity of modifications in the first 20–30 nt, with the two separate ligation steps ensuring that any truncated fragments formed due to polymerase fall-off during reverse transcription, as a result of secondary structure or modified ribonucleosides, would still be amplified during the PCR step. The tRNA-seq method revealed that most sequencing reads were 61–70 nt in length (70 nt sequencing maximum) and that mutation rates were higher than simple polymerase errors, suggesting successful polymerase read-through for most modified ribonucleosides.

Another important conclusion is that the tRNA-seq method is quantitatively robust, with high precision over a 10^6 -fold dynamic range (0.8–242 000 counts per million), which allows significant distinctions to be made among relatively small changes in tRNA copy number. In six biological replicates of three treatment conditions, the coefficient of variation (CV) for absolute read counts of the 76 tRNA species averaged 0.41 ± 0.06 (mean \pm S.D.) over this dynamic range on the HiSeq and 0.52 ± 0.09 for MiSeq, while small RNA samples displayed CVs of 0.27 ± 0.11 and 0.24 ± 0.05 for HiSeq and MiSeq, respectively (Supplementary Information Table S2). This precision allowed significant ($P < 0.05$) resolution of stress-induced changes in tRNA levels as low as 1.4-fold, which has not been possible by other methods.

The tRNA sequencing method provides other significant advantages over existing tRNA profiling techniques, including the extant RNA-seq approaches discussed earlier and tRNA microarrays (14). Similar to comparisons of RNA-seq to microarrays for transcriptional profiling, a major advantage of the tRNA sequencing technology over tRNA microarrays lies in the simultaneous analysis of many tRNA samples from the same or different organisms in a single lane in the sequencer compared to a single microarray for each tRNA sample and different microarrays for different organisms. Current microarray technology is limited to a subset of 39 of the 56 uniquely expressed cytoplasmic tRNA species in *S. cerevisiae*, with the requirement for a minimum 10 bp difference making it impossible to distinguish many isodecoders (15). Combined with the larger dynamic range of tRNA sequencing (10^6 versus 10^2 for microarrays) (15), tRNA-seq offers greater versatility in the information derived from a single analysis, with simultaneous tRNA profiling, fragment analysis and modification-induced mismatch data.

Although rigorously quantitative and versatile, tRNA-seq is not without limitations. As discussed previously, the ligation and PCR amplification steps are likely the cause of the wide range of read counts and the 'jackpotting' (44) observed for several tRNAs, which limits absolute quantification of tRNAs in a sample. The power of tRNA-seq lies in the sensitive and precise quantification of changes in tRNA abundance as a function of environmental changes, as part of a larger translational control system in the cell stress response. Improvements in ligation efficiency could enhance absolute quantification of tRNA species, but the combination of PCR idiosyncrasies and the fact that even the best reported ligation efficiency of 95% still introduces significant inaccuracies during PCR amplification make rigorous

absolute quantification unreliable for all forms of RNA sequencing.

There are many applications of the tRNA-seq method in systems-level analyses of changes in tRNA abundance in translation biology, such as the role of tRNA levels in the efficient translation of optimal synonymous codons in genes (17). Here, we applied tRNA-seq to quantify stress-induced changes in tRNA levels to define the role of tRNA abundance in translational control of the cell stress response. We recently discovered that cells respond to a stress by altering the levels of the dozens of modified ribonucleosides in tRNA, with a unique pattern of altered tRNA modification levels for each different stress (9–11). For example, H₂O₂ exposure increased the levels of m⁵C, m²G and Cm, while these modifications remained unchanged or decreased in cells exposed to MMS (11). The observed increase in a tRNA modification could result from increased enzymatic activity, an increase in the number of copies of one or more tRNAs, or both, which raises the question of the potential for analogous stress-specific patterns of altered levels of tRNA species. Furthermore, stress-induced reprogramming of modifications was found to affect specific wobble modifications, which led to selective translation of mRNAs enriched with the cognate codons for the wobble-modified tRNAs (9–11). These mRNAs code for critical stress response proteins derived from families of codon-based genes (9–11). Again, tRNA-seq was used to assess the role of tRNA levels in driving this codon-biased translation.

The tRNA-seq data reveal that both oxidation and alkylation stresses caused significant changes ($P < 0.1$) in the levels of less than half of the tRNAs, while levels varied by up to 4-fold for those tRNAs for which either stress caused a significant change (Supplementary Table S3). Hierarchical cluster analysis revealed strikingly consistent trends of up- or down-regulation for all but 18 of the tRNAs (Figure 3), which suggests that changes in the levels of most tRNAs are independent of the identity of the stress and may represent a nonspecific stress response. However, 18 tRNAs showed stress-specific behavior, with opposing changes for H₂O₂ and MMS exposures (Figure 3). Thus, like the stress-specific reprogramming of a subset of the 25 tRNA modifications spread across all tRNAs, a subset of expressed tRNAs also shows toxicant-specific behaviors. In at least one instance, this correlation is consistent with the idea of coordinated regulation of stress-altered ribonucleoside modifications and tRNA copy numbers. In *S. cerevisiae* exposed to H₂O₂, the level of m⁵C at the wobble position of tRNA^{Leu(CAA)} increased by 1.7-fold and enhanced the translation of proteins from genes enriched in the cognate codon, TTG (10). tRNA-seq revealed that H₂O₂ exposure also caused a 1.8-fold increase in the number of copies of tRNA^{Leu(CAA)} ($P < 0.05$). This may represent a mechanism to amplify the translation-enhancing effects of a wobble m⁵C in tRNA^{Leu(CAA)}. However, this correlation could also be a coincidence, as suggested by the example of the mcm⁵U modification at the wobble position of tRNA^{Arg(U^{CU})}, which is increased following exposure of *S. cerevisiae* to MMS (9). In this case, the number of copies of tRNA^{Arg(U^{CU})} did not increase significantly (1.2-fold-change, $P = 0.46$) (Supplementary Table S3). Interestingly, the level of this tRNA increased significantly (2.2-fold, $P < 0.005$) following H₂O₂

exposure (Supplementary Table S3). An analysis of Supplementary Table S3 also reveals that there is no correlation between tRNAs for optimal codons (i.e. the most frequently used codons in the yeast genome) and any stress-specific up- or down-regulation. Taken together, these data do not rule out the possibility that tRNA modifications and tRNA abundance are coordinately controlled during stress responses, but instead suggest that, for the majority of tRNAs, stress-induced changes in tRNA modifications are independent of changes in tRNA abundance. As discussed next, consideration of the various known tRNA degradation pathways supports this conclusion, though further clarification of the relationship between tRNA modifications and tRNA abundance is needed.

There is emerging appreciation for a variety of mechanisms that degrade tRNAs in RNA maturation quality control processes and during cell stress. These pathways include two involved in tRNA maturation and quality control: the rapid tRNA decay (RTD) pathway, in which tRNAs lacking the m⁷G, m⁵C, Um and ac⁴C modifications are selectively degraded (6), and the TRAMP/Rrp6-mediated tRNA degradation pathway, in which tRNAs are subjected to degradation in the nuclear exosome (7). There are also stress-induced degradation pathways involving ribonuclease-induced cleavage of tRNA in its anticodon loop (3,4) or D-loop (45). While all of these degradation mechanisms could contribute to the changes in tRNA abundance observed here in the yeast alkylation and oxidation stress responses, the results obtained with the tRNA-seq method suggest that our understanding of tRNA degradation pathways is incomplete. The tRNA-seq data suggest that the observed stress-induced changes in the tRNA copy numbers are, to a large extent, independent of the stress-induced degradation of tRNAs observed in other published studies (3,4,7,35), which is consistent with different functions for the two phenomena. While the oxidative and alkylation stresses induced here caused about 25% of the tRNAs to decrease by 30% or more (and up to 75% for several; Supplementary Table S3), our results are consistent with published observations of tRNA fragmentation by oxidative stress, which show negligible changes in the quantity of the affected tRNA (4) and suggest a signaling or control function for the tRNA fragments (3,4,35). As such, the bulk of our sequencing reads represent full-length tRNA, with truncated reads resulting from reverse transcriptase fall-off due to base modifications or secondary structure of the tRNA. In addition, it has been shown that defects in tRNA nuclear export do not significantly affect global protein synthesis, as reduced pools of tRNA in the cytoplasm are sufficient to maintain efficient translation (46). Another study also showed that increased levels of a low-abundance tRNA had no effect on translation (47), again suggesting that cells transcribe tRNA in excess of what is required for cytoplasmic-based protein synthesis (46). Taken together, the data suggest that mass degradation of tRNAs or large-scale increases and decreases in tRNA levels in a cell are not the only factors in translational control of gene expression. Moreover, >50% of yeast tRNAs harbor the m⁷G and m⁵C modifications that have been shown to play a protective function against degradation at the 5'-end of tRNA by the RTD pathway during stress (6,48,49),

with the quantity of these modifications either increased or unchanged in tRNAs during the oxidation and alkylation stress responses (10,11). These methylation-based modifications work toward preventing large-scale degradation of these tRNAs while allowing them to remain intact for translation of other stress-response proteins (1). Recently, it was discovered that angiogenin, the ribonuclease that cleaves tRNAs under stress conditions in mammalian cells (3), cleaves first within the 3'-CCA terminus of all tRNAs in order to block aminoacylation of tRNAs (38). Unlike the anticodon loop cleavage of tRNAs into halves, this cleavage at the CCA end occurred in all tRNAs and on a much faster time scale. Consistent with these findings, our untargeted analysis of small RNA species revealed that neither H₂O₂ nor MMS stress caused large-scale degradation detectable as either significant loss of parent tRNA species or increases in tRNA fragments between 20 and 40 nt in length (Supplementary Figure S5a). However, one tRNA species previously shown to undergo oxidative stress-induced anticodon loop cleavage into half tRNAs in *S. cerevisiae*, tRNA^{Met(CAU)}, also showed a non-significant 1.4-fold increase in 31–40 nt tRNA fragments in our studies (Supplementary Figure S5b). Interestingly, the level of full-length tRNA^{Met(CAU)} did not change during oxidative stress, which is consistent with previous studies (37). It is also possible that larger changes in the total level of each tRNA species might mask the relatively small changes in degradation levels. Refinement of the tRNA-seq method with optimized ligation conditions will be required to make this tRNA sequencing method more quantitative for tRNA degradation products.

One interesting feature revealed by the tRNA-seq data was the observation of differential control of tRNA levels for pairs of isodecoders partitioned between mitochondria and nucleus. Specifically, there are four tRNA isodecoder pairs for which one member is cytoplasmic and the other is mitochondrial, with one of the pair increasing in response to a specific stress and the other decreasing (Supplementary Figure S6). This is consistent with previous data indicating that isoacceptors of the same tRNA could have very different cleavage profiles under the same stress conditions (36). Differential regulation of abundances for the same isoacceptors in the cytosol and mitochondria would allow separate translational control of specific mitochondrial and cytoplasmic stress response proteins, which would not be surprising in light of the important role of mitochondrial tRNAs in many human diseases (50). Taken together, this also supports previous work suggesting that tRNA isodecoders may have distinct functions and perhaps activities unrelated to translation (28).

In summary, this tRNA sequencing method exploits the paucity of ribonucleoside modifications at the 3'-end of tRNAs to identify and quantify all expressed tRNA species in a cell, with application to cells subjected to two chemical stresses revealing both stress-specific and nonspecific changes in tRNA levels in the translational control of stress response.

SUPPLEMENTARY DATA

Supplementary Data are available at NAR Online.

ACKNOWLEDGMENT

We thank the MIT BioMicro Center staff for technical advice regarding sample preparation for Illumina sequencing.

FUNDING

National Institutes of Health [ES017010 and ES002109]; National Science Foundation [CHE-1308839]; National Research Foundation of Singapore under its Singapore-MIT Alliance for Research and Technology. Funding for open access charge: National Institutes of Health [ES017010 and ES002109]; National Science Foundation [CHE-1308839]; National Research Foundation of Singapore under its Singapore-MIT Alliance for Research and Technology.

Conflict of interest statement. None declared.

REFERENCES

- Phizicky, E.M. and Hopper, A.K. (2010) tRNA biology charges to the front. *Genes Dev.*, **24**, 1832–1860.
- Machnicka, M.A., Milanowska, K., Osman Oglou, O., Purta, E., Kurkowska, M., Olchowik, A., Januszewski, W., Kalinowski, S., Dunin-Horkawicz, S., Rother, K.M. *et al.* (2013) MODOMICS: a database of RNA modification pathways—2013 update. *Nucleic Acids Res.*, **41**, D262–D267.
- Yamasaki, S., Ivanov, P., Hu, G.F. and Anderson, P. (2009) Angiogenin cleaves tRNA and promotes stress-induced translational repression. *J. Cell Biol.*, **185**, 35–42.
- Thompson, D.M. and Parker, R. (2009) Stressing out over tRNA cleavage. *Cell*, **138**, 215–219.
- Wilusz, J.E., Whipple, J.M., Phizicky, E.M. and Sharp, P.A. (2011) tRNAs marked with CCACCA are targeted for degradation. *Science*, **334**, 817–821.
- Chernyakov, I., Whipple, J.M., Kotelawala, L., Grayhack, E.J. and Phizicky, E.M. (2008) Degradation of several hypomodified mature tRNA species in *Saccharomyces cerevisiae* is mediated by Met22 and the 5'-3' exonucleases Rat1 and Xrn1. *Genes Dev.*, **22**, 1369–1380.
- Wichtowska, D., Turowski, T.W. and Boguta, M. (2013) An interplay between transcription, processing, and degradation determines tRNA levels in yeast. *WIREs RNA*, **4**, 709–722.
- Agris, P.F., Vendeix, F.A. and Graham, W.D. (2007) tRNA's wobble decoding of the genome: 40 years of modification. *J. Mol. Biol.*, **366**, 1–13.
- Begley, U., Dyavaiah, M., Patil, A., Rooney, J.P., DiRenzo, D., Young, C.M., Conklin, D.S., Zitomer, R.S. and Begley, T.J. (2007) Trm9-catalyzed tRNA modifications link translation to the DNA damage response. *Mol. Cell*, **28**, 860–870.
- Chan, C.T., Pang, Y.L., Deng, W., Babu, I.R., Dyavaiah, M., Begley, T.J. and Dedon, P.C. (2012) Reprogramming of tRNA modifications controls the oxidative stress response by codon-biased translation of proteins. *Nat. Commun.*, **3**, 937.
- Chan, C.T., Dyavaiah, M., DeMott, M.S., Taghizadeh, K., Dedon, P.C. and Begley, T.J. (2010) A quantitative systems approach reveals dynamic control of tRNA modifications during cellular stress. *PLoS Genet.*, **6**, e1001247.
- Bauer, F. and Hermand, D. (2012) A coordinated codon-dependent regulation of translation by Elongator. *Cell Cycle*, **11**, 4524–4529.
- Begley, T.J., Rosenbach, A.S., Ideker, T. and Samson, L.D. (2004) Hot spots for modulating toxicity identified by genomic phenotyping and localization mapping. *Mol. Cell*, **16**, 117–125.
- Dittmar, K.A., Mobley, E.M., Radek, A.J. and Pan, T. (2004) Exploring the regulation of tRNA distribution on the genomic scale. *J. Mol. Biol.*, **337**, 31–47.
- Dittmar, K.A., Goodenbour, J.M. and Pan, T. (2006) Tissue-specific differences in human transfer RNA expression. *PLoS Genet.*, **2**, e221.
- Zaborske, J.M., Narasimhan, J., Jiang, L., Wek, S.A., Dittmar, K.A., Freimoser, F., Pan, T. and Wek, R.C. (2009) Genome-wide analysis of tRNA charging and activation of the eIF2 kinase Gcn2p. *J. Biol. Chem.*, **284**, 25254–25267.

17. Tuller, T., Carmi, A., Vestsgian, K., Navon, S., Dorfan, Y., Zaborske, J., Pan, T., Dahan, O., Furman, I. and Pilpel, Y. (2010) An evolutionarily conserved mechanism for controlling the efficiency of protein translation. *Cell*, **141**, 344–354.
18. Wang, Z., Gerstein, M. and Snyder, M. (2009) RNA-Seq: a revolutionary tool for transcriptomics. *Nat. Rev. Genet.*, **10**, 57–63.
19. Ebhardt, H.A., Tsang, H.H., Dai, D.C., Liu, Y., Bostan, B. and Fahlman, R.P. (2009) Meta-analysis of small RNA-sequencing errors reveals ubiquitous post-transcriptional RNA modifications. *Nucleic Acids Res.*, **37**, 2461–2470.
20. Iida, K., Jin, H. and Zhu, J.K. (2009) Bioinformatics analysis suggests base modifications of tRNAs and miRNAs in *Arabidopsis thaliana*. *BMC Genomics*, **10**, 155.
21. Cai, P., Piao, X., Hao, L., Liu, S., Hou, N., Wang, H. and Chen, Q. (2013) A deep analysis of the small non-coding RNA population in *Schistosoma japonicum* eggs. *PLoS One*, **8**, e64003.
22. Bentley, D.R., Balasubramanian, S., Swerdlow, H.P., Smith, G.P., Milton, J., Brown, C.G., Hall, K.P., Evers, D.J., Barnes, C.L., Bignell, H.R. *et al.* (2008) Accurate whole human genome sequencing using reversible terminator chemistry. *Nature*, **456**, 53–59.
23. Chionh, Y.H., Ho, C.H., Pruksakorn, D., Ramesh Babu, I., Ng, C.S., Hia, F., McBee, M.E., Su, D., Pang, Y.L., Gu, C. *et al.* (2013) A multidimensional platform for the purification of non-coding RNA species. *Nucleic Acids Res.*, **41**, e168.
24. Chan, P.P. and Lowe, T.M. (2009) GtRNAdb: a database of transfer RNA genes detected in genomic sequence. *Nucleic Acids Res.*, **37**, D93–D97.
25. Kent, W.J. (2002) BLAT—the BLAST-like alignment tool. *Genome Res.*, **12**, 656–664.
26. Robinson, M.D., McCarthy, D.J. and Smyth, G.K. (2010) edgeR: a bioconductor package for differential expression analysis of digital gene expression data. *Bioinformatics*, **26**, 139–140.
27. Goodenbour, J.M. and Pan, T. (2006) Diversity of tRNA genes in eukaryotes. *Nucleic Acids Res.*, **34**, 6137–6146.
28. Geslain, R. and Pan, T. (2010) Functional analysis of human tRNA isodecoders. *J. Mol. Biol.*, **396**, 821–831.
29. Day, D.S., Luquette, L.J., Park, P.J. and Kharchenko, P.V. (2010) Estimating enrichment of repetitive elements from high-throughput sequence data. *Genome Biol.*, **11**, R69.
30. Bissels, U., Wild, S., Tomiuk, S., Holste, A., Hafner, M., Tuschl, T. and Bosio, A. (2009) Absolute quantification of microRNAs by using a universal reference. *RNA*, **15**, 2375–2384.
31. Zhang, Z., Lee, J.E., Riemondy, K., Anderson, E.M. and Yi, R. (2013) High-efficiency RNA cloning enables accurate quantification of miRNA expression by deep sequencing. *Genome Biol.*, **14**, R109.
32. Ryvkin, P., Leung, Y.Y., Silverman, I.M., Childress, M., Valladares, O., Dragomir, I., Gregory, B.D. and Wang, L.S. (2013) HAMR: high-throughput annotation of modified ribonucleotides. *RNA*, **19**, 1684–1692.
33. Loman, N.J., Misra, R.V., Dallman, T.J., Constantinidou, C., Gharbia, S.E., Wain, J. and Pallen, M.J. (2012) Performance comparison of benchtop high-throughput sequencing platforms. *Nat. Biotechnol.*, **30**, 434–439.
34. Dey, B.K., Mueller, A.C. and Dutta, A. (2012) Non-micro-short RNAs: the new kids on the block. *Mol. Biol. Cell*, **23**, 4664–4667.
35. Ivanov, P., Emara, M.M., Villen, J., Gygi, S.P. and Anderson, P. (2011) Angiogenin-induced tRNA fragments inhibit translation initiation. *Mol. Cell*, **43**, 613–623.
36. Saikia, M., Krokowski, D., Guan, B.J., Ivanov, P., Parisien, M., Hu, G.F., Anderson, P., Pan, T. and Hatzoglou, M. (2012) Genome-wide identification and quantitative analysis of cleaved tRNA fragments induced by cellular stress. *J. Biol. Chem.*, **287**, 42708–42725.
37. Thompson, D.M., Lu, C., Green, P.J. and Parker, R. (2008) tRNA cleavage is a conserved response to oxidative stress in eukaryotes. *RNA*, **14**, 2095–2103.
38. Czech, A., Wende, S., Morl, M., Pan, T. and Ignatova, Z. (2013) Reversible and rapid transfer-RNA deactivation as a mechanism of translational repression in stress. *PLoS Genet.*, **9**, e1003767.
39. Lee, Y.S., Shibata, Y., Malhotra, A. and Dutta, A. (2009) A novel class of small RNAs: tRNA-derived RNA fragments (tRFs). *Genes Dev.*, **23**, 2639–2649.
40. Mutz, K.O., Heilkenbrinker, A., Lonne, M., Walter, J.G. and Stahl, F. (2013) Transcriptome analysis using next-generation sequencing. *Curr. Opin. Biotechnol.*, **24**, 22–30.
41. Alon, S., Vigneault, F., Eminaga, S., Christodoulou, D.C., Seidman, J.G., Church, G.M. and Eisenberg, E. (2011) Barcoding bias in high-throughput multiplex sequencing of miRNA. *Genome Res.*, **21**, 1506–1511.
42. Hafner, M., Renwick, N., Brown, M., Mihailovic, A., Holoch, D., Lin, C., Pena, J.T., Nusbaum, J.D., Morozov, P., Ludwig, J. *et al.* (2011) RNA-ligase-dependent biases in miRNA representation in deep-sequenced small RNA cDNA libraries. *RNA*, **17**, 1697–1712.
43. Emmerechts, G., Barbe, S., Herdewijn, P., Anne, J. and Rozenski, J. (2007) Post-transcriptional modification mapping in the *Clostridium acetobutylicum* 16S rRNA by mass spectrometry and reverse transcriptase assays. *Nucleic Acids Res.*, **35**, 3494–3503.
44. Linsen, S.E., de Wit, E., Janssens, G., Heater, S., Chapman, L., Parkin, R.K., Fritz, B., Wyman, S.K., de Bruijn, E., Voest, E.E. *et al.* (2009) Limitations and possibilities of small RNA digital gene expression profiling. *Nat. Methods*, **6**, 474–476.
45. Murakami, S., Fujishima, K., Tomita, M. and Kanai, A. (2012) Metatranscriptomic analysis of microbes in an oceanfront deep-subsurface hot spring reveals novel small RNAs and type-specific tRNA degradation. *Appl. Environ. Microbiol.*, **78**, 1015–1022.
46. Chu, H.Y. and Hopper, A.K. (2013) Genome-wide investigation of the role of the tRNA nuclear-cytoplasmic trafficking pathway in regulation of the yeast *Saccharomyces cerevisiae* transcriptome and proteome. *Mol. Cell Biol.*, **33**, 4241–4254.
47. Letzring, D.P., Dean, K.M. and Grayhack, E.J. (2010) Control of translation efficiency in yeast by codon-anticodon interactions. *RNA*, **16**, 2516–2528.
48. Alexandrov, A., Chernyakov, I., Gu, W., Hiley, S.L., Hughes, T.R., Grayhack, E.J. and Phizicky, E.M. (2006) Rapid tRNA decay can result from lack of nonessential modifications. *Mol. Cell*, **21**, 87–96.
49. Alexandrov, A., Martzen, M.R. and Phizicky, E.M. (2002) Two proteins that form a complex are required for 7-methylguanosine modification of yeast tRNA. *RNA*, **8**, 1253–1266.
50. Konovalova, S. and Tyynismaa, H. (2013) Mitochondrial aminoacyl-tRNA synthetases in human disease. *Mol. Genet. Metab.*, **108**, 206–211.